

Numerical analysis and modelling of recirculating flows

Christina G. Georgantopoulou, George A. Georgantopoulos and
Nikolaos S. Vasilikos

Abstract---One of the most important issues in control engineering of flows is the accurate specification of recirculating zones, especially at various fluid and thermal industrial applications, where the working fluid's pressure and temperature values are important enough. In the present paper we develop a complete numerical approach for the simulation, modeling and estimation of recirculating flows, mainly inside short pipes. We use Cartesian grids, uniform as well as structured – nested ones with refinement, in order to succeed the appropriate choice of the number of sub-grids and the refinement factor providing accurate results for the fluid flow. The mathematical modeling of the governing Navier – Stokes equations consist of upwind schemes with up to third order of accuracy. We present the incompressible, steady and laminar flow inside a square lid-driven cavity, a channel with step and a backward facing step channel, trying to predict the recirculation lengths and define the position of detachment and reattachment points. The utility of the methodology is tested by comparing our results to those of the standard single algorithm as well as of the literature. We conclude that our numerical algorithms and technique provide accurate results for the prediction of the recirculating incompressible flows and it can be applied in extended pipeline flow networks.

Keywords---*incompressible flow, recirculating flows, refinement techniques, viscous flow*

I. INTRODUCTION

THE circulating flows present great interest due to the various industrial applications in engineering flow processes. An accurate but also a simple numerical technique for the simulation and estimation of these flows can contribute in pressure control and safety issues or in thermal cycle's efficiency improvement. Many accurate approaches have been done, as Louda's [1,2] where a numerical approach for backward facing steps is presented giving detailed results, or Wallin's methodology [3] and Torres's [4] for turbulent flows with interesting recirculating zones in short pipes.

Chr.G.Georgantopoulou was with National Technical University of Athens and Harokopio University, while now she is with the School of Engineering, Bahrain Polytechnic, PO Box 33349, Isa Town, Kingdom of Bahrain (corresponding author; email: christina@polytechnic.bh)
G.A.Georgantopoulos is with Hellenic Air Force Academy, Dekeleia Attikis, Greece (email: gageorgant@yahoo.gr)
N.S.Vasilikos is with School of Pedagogical and Technological Education, Irakleion Attikis, Greece (email: vasnikoler@yahoo.gr)

Very interesting experimental approaches have been developed for various flows with recirculation by Lee [5] or Armaly [6] and Willis [7], as well as various numerical approaches for backward facing steps [8,9,10]. Cartesian grids seem to be the most appropriate for the case of recirculating flows in pipes, because in most of the cases the curvilinear or complex part of the physical domains are limited. Using appropriate methodologies this type of grids can also be used for the numerical simulation and discretization of domains with complex geometrical bounds producing very satisfied results. The main advantage is that the specification of the geometry description is simple, using most of the times only grid lines. [11], [12].

Although most of the Cartesian generation techniques are independent of the domain shape and dimensions, there are some cases where a huge number of Cartesian cells have to be used if we want to produce accurate results. For example in the case of oil pipeline flows, it is almost impossible to use only uniform Cartesian grids because the computational memory and time will be increased in an inappropriate level. This is the main reason that various refinement mesh techniques have been developed overcoming the huge number of cells, which some physical domains demand for the numerical simulation. The refinement approaches are based on cell – refinement either on region – refinement according some specific criteria. Many approaches have been developed regarding adaptive or mesh refinement techniques. Wang [13] proposes a quad tree-based adaptive Cartesian/Quadrilateral grid generator and flow solver based on cell cutting-[14], [15], Lee [16] presents an numerical scheme based on cutting cells for Turbulent flows using Cartesian grids and Pan [17] a ghost cell method for incompressible flows.

Various approaches have been presented regarding the implementation of the boundary conditions, although most of the times we enforce the value of one variable and we solve for the others. A method where the velocity is enforced, is presented by Faldun [18], where the boundary conditions are applied to the nearest nodes of the physical boundary. Ikeno [19] uses a pressure correction scheme, where the pressure gradient at boundary nodes can modify the enforced velocity value, while Tseng [20], presents a very interesting approach for the immersed boundary method, which can be probably applied in complex curvilinear geometries with satisfied convergence of the numerical algorithm.

In the present paper a Cartesian grid generation algorithm is used in combination with upwind schemes for the equations' solution in order to obtain the characteristics

of recirculating incompressible laminar flows. Particular interest will be given in the identification of the recirculation lengths as well as the reduction of the computational time according to the appropriate refinement technique. In order to create the approximated Cartesian bounds of the physical domains we develop a method using only grid lines, [21],[22] based on Chen, Lee and Patakar [16]. We also develop a refinement methodology using structured sub-grids [23], based on grid generation criteria of Martin and Collela [11], and Berger and Collela [24]. The numerical solution of Navier –Stokes equations is based on an artificial compressibility technique [25]. Three different cases will be presented with extended recirculating regions, giving particular emphasis to the accuracy and the convergence of the results, trying to specify the recirculation length and the important points regarding each particular flow field and trying also to prove that our numerical approach provides accurate results for the flows with recirculating regions. Particular investigation is taken place concerning the nested refinement technique, trying to improve the accuracy of the results and reducing the computational memory and time simultaneously.

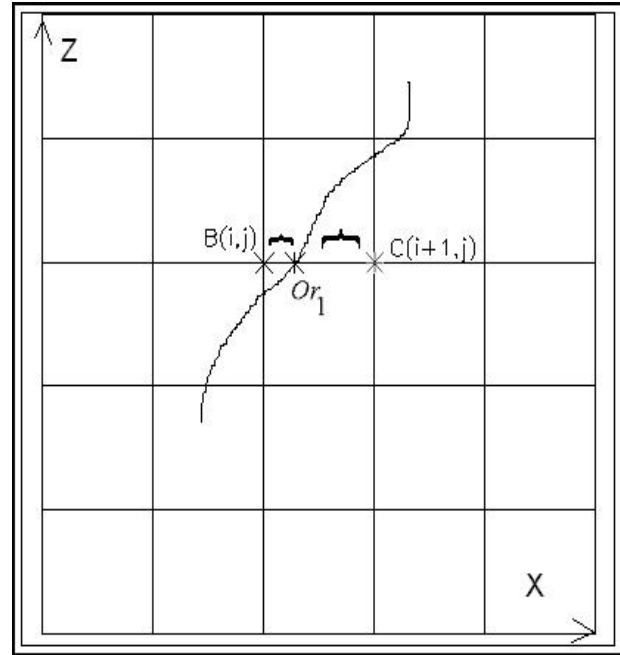


Fig. 1: Specification of approximate Cartesian points

II. MATHEMATICAL MODELING AND NUMERICAL SOLUTION

The numerical approach of flow fields consists of several steps, where plenty of methods can be applied. Especially at the cases of recirculation regions a precise way of geometry description is needed in order to ensure the flow rate conservation and predict the lengths as well as the important points with accuracy. The method which we propose is independent of the physical geometry description and it can be applied even if a complex curvilinear bound has to be approached. At the following sections each step of our numerical methodology is presented concerning the physical domain simulation, the numerical solution of the governing equations, the application of the boundary conditions as well as the best numerical approach for the recirculation zones. Various applications using several methodologies have been developed for the prediction of circulating flows [26, 27, and 28]

A. Physical domain discretization

In our numerical approach, if the physical domain bounds are aligned with Cartesian grid lines, we have no need to produce any approximated bound. However, if our domain consists of complex or curvilinear bounds, we have to create a new approximated one in order to proceed to the grid generation. [12] The new approximate bound is parted only by the use of grid lines, on x or z-axis either and this is our benefit. The method is used, called saw-tooth and is has been chosen as the most appropriate for the finite volume cell centered numerical simulation of flow fields. This method provides independence and automation of grid generation for problems with complex boundaries, with or without existence of an analytical function. The new geometrical approach is based on sets of data points, the original points as well as the approximated points of the body contour as we describe below.

Consequently, the first step is the creation of a new approximated Cartesian bound of our physical domain. We project the original contour of the curvilinear geometry onto a Cartesian grid. This complex contour is described by a set of data points on x or z-axis either. We have to control if the contour segment between two neighbour data points varies monotonically with respect to both x or z directions. If we discover that this rule doesn't occur we have to cluster the Cartesian grid and repeat the above procedure. In order to define the new approximated points we follow the below rule: if an original data point is on x-axis, we calculate the distance between this and its neighbouring grid nodes in the same direction (x). According the smallest distance we choose the corresponding grid node as the Cartesian approximated point, (fig. 1). By this way we define the new points, applying the rule of minimum distance for each set of original data points. We finally connect the new points using only grid lines (saw-tooth method), (fig. 2)

B. Mesh generation and refinement technique

As we have fulfilled the above procedure, we can create a Cartesian grid, excluding the cells that there are no more included to the flow field due to the above approximation. Therefore a new Cartesian grid is generated where all the "new physical" bounds lie on grid lines.

Although most of the times the above grid generation technique is appropriate for the solution, sometimes a huge number of cells is needed in order to simulate the whole physical domain. That is why we develop a block refinement technique by the use of a hierarchical structured grid approach. The method is based on using a sequence of nested rectangular meshes in which numerical simulation is taking place (fig. 3). The whole domain is a rectangle whose sides lie in the coordinate directions. We simulate the domain based in as many refine grids as we need. [23]. At the case of recirculating flows inside pipes (short or extended), the above block nested refinement is more appropriate method than others, because the sub grids are

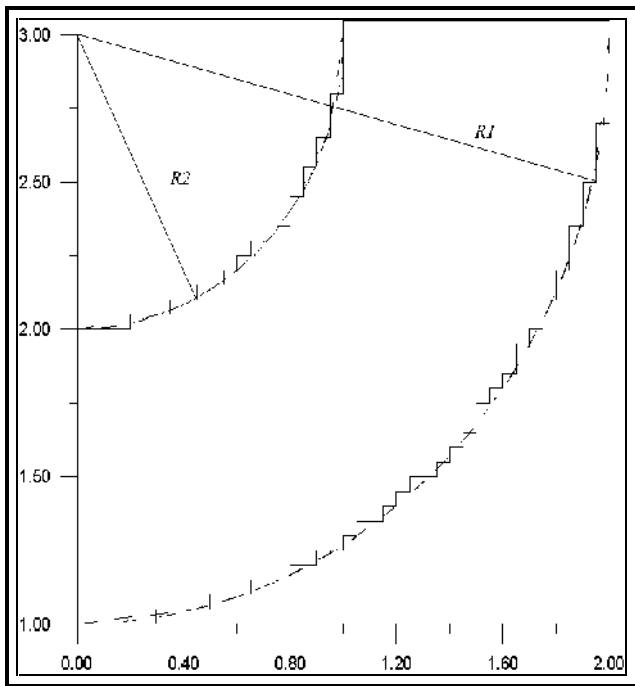


Fig. 2: Method for the connection of the Cartesian approximated points (saw-tooth)

simply created in any region we demand, without any complicated adaptive techniques, using simultaneously the refinement factor that each case demands. By the other hand, we prefer to propose easy specification of our grid adaptation, which will provide simple and accurate results in many industrial applications. In the case of recirculating flows, a refinement technique is absolutely necessary in order to avoid huge number of cells which are created (i.e. at the case of pipe's gas flows) and by the other hand to estimate the related lengths, points as well variables with accuracy. Especially in extended pipeline networks, low interest is presented at the straight parts of these, where the domain discretization can be occurred using uniform Cartesian grids developing the minimum number of cells. At the regions with curvilinear bounds, the block nested refinement technique can be easily applied providing better accuracy and reducing the computational time simultaneously. In this method the refinement is convenient to be a power of 2.

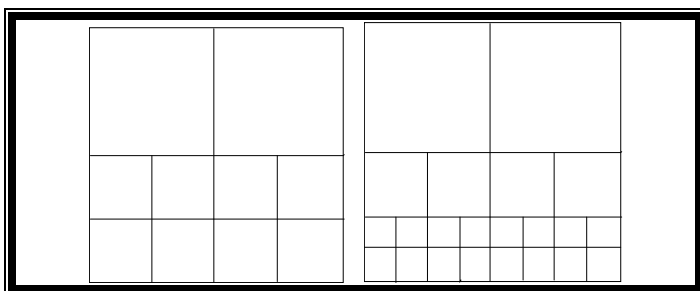


Fig. 3: Block nested refinement, grid levels=2 and refinement factor = 2

The proposed nested algorithm contains several levels of grids. We name the coarsest level $m=0$ and each next refine sub – grid is named $m+1$. We define an integer refinement factor:

$$I = dx_m / dx_{m+1} = dz_m / dz_{m+1}. \quad (1)$$

As we have created the coarse grid we simulate the flow field and calculate the variables. At this time the coarse-fine interfaces are neglected since no information from the finer level is available yet. We have already defined the limits of the refinement levels and we proceed the calculation to the next refinement level. The sub-grids bounds must lie on a grid line of the previous level grid. As we use staggered grids and the variable values are expressed on the cell's center, we consider pseudo – cells (artificial cells), all around the physical domain and the sub – grids too. (fig. 4) By this way we estimate the variables using interpolation between pseudo – cells and their neighbor cells for the velocity value. The pseudo-cells of each sub-grid m are lying on the level $m-1$. We continue this process for all the sub- grids.

As we have fulfilled the simulation in all sub-grids and we have the flow field results at m_{max} level, we resolve the problem in the coarser levels again to ensure conservation. We find a new solution, this time by the influence of the fine levels. In addition we must satisfy both Dirichlet and Neumann matching conditions along coarse-fine and fine-coarse interfaces. That's why we give the velocity values, but we solve for pressure. With nested grids, each grid is separately defined and has its own solution vector, so that a grid can be advanced independently of other grids, except for the determination of its boundary values. The information exchange between two successive levels is described in the next section.

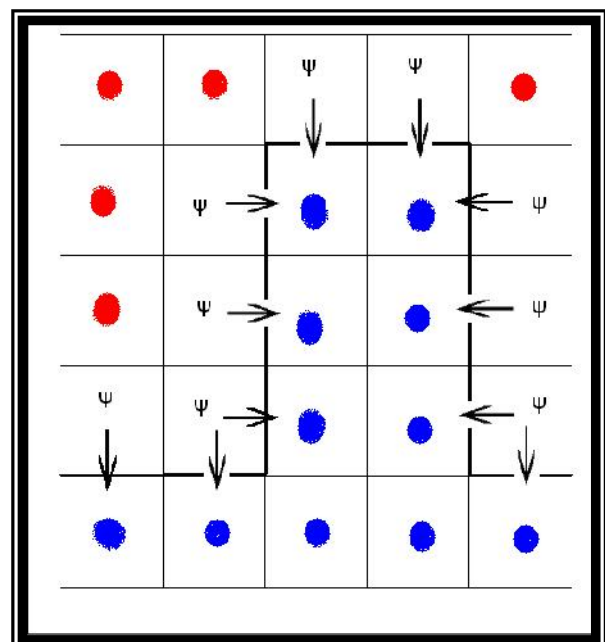


Fig 4: Ways of boundary conditions application. The red cells are excluded by the flow field, while the blue cells are included in it. ψ : artificial cells

Let's consider that we have already solved into the initial coarse grid and we have to continue the numerical simulation into a sub-grid. In order to specify the boundary conditions at coarse grid and sub-grid interfaces, we represent $u^{m+1}(i,k)$ and $w^{m+1}(i,k)$, the values of the velocity components on the sub-grid pseudo-cells. The $u^m(l,n)$ and $w^m(l,n)$ are the corresponding coarse grid values into the physical domain. Every interpolation takes place either on x either on y- axis. If we consider that we apply the new velocity values on x-axis, (figure 3), interpolation is applied as follows:

$$u^{m+1}(i,k) = \frac{u^m(l,n) + u^m(l+1,n)}{2} \quad (2)$$

and

$$w^{m+1}(i,k) = \frac{w^m(l,n) + w^m(l+1,n)}{2} \quad (3)$$

Also,

$$u^{m+1}(i,k) = u^{m+1}(i+1,k) = \dots = u^{m+1}(i+I-1,k) \quad (4)$$

Concerning the pressure boundary condition, we prefer not to apply interpolation and develop a different approach for this variable. Assuming that we simulate for an axisymmetric flow, the pressure vertical derivative at the interface is estimated as follows:

$$\begin{aligned} \frac{\partial p}{\partial n} = & n_x \left[\frac{1}{\text{Re}} \left(\frac{\partial^2 u}{\partial y^2} + \frac{1}{y} \cdot \frac{\partial u}{\partial y} + \frac{\partial^2 u}{\partial x^2} \right) - u \cdot \frac{\partial u}{\partial x} - v \cdot \frac{\partial u}{\partial y} \right] + \\ & + n_y \left[\frac{1}{\text{Re}} \left(\frac{\partial^2 v}{\partial y^2} + \frac{1}{y} \cdot \frac{\partial v}{\partial y} + \frac{\partial^2 v}{\partial x^2} - \frac{v}{y^2} \right) - u \cdot \frac{\partial v}{\partial x} - v \cdot \frac{\partial v}{\partial y} \right] \end{aligned} \quad (5)$$

In fact, we can apply liner interpolation for both of the above flow variables, but if we want to develop an non - depended technique which can be apply to a wide range of various applications [28],[29], we prefer to solve for the pressure by the above way or an alternative one. Most of the researchers prefer this option. [23]

C. Governing Equations and Numerical Scheme

The incompressible governing flow equations are the Navier-Stokes equations, which, expressed in terms of the Cartesian system of coordinates (x, z) , and using the above relations for time derivatives, take the form:

$$[\Gamma] \frac{\partial q}{\partial t} + \frac{\partial e}{\partial x} + \frac{\partial g}{\partial z} + r \cdot \frac{g_1}{z} = \frac{1}{\text{Re}} \left(\frac{\partial}{\partial x} + \frac{\partial s}{\partial z} + r \cdot \frac{s_1}{z} \right) \quad (6)$$

Where, $[\Gamma] = \text{diag}(0,1,1)$ is the singular diagonal matrix, a is a switch for the activation of the axisymmetric terms ($=0$ is

non axisymmetric, $a=1$ axisymmetric flow field), Re the Reynolds number and Q the unknown solution vector, $Q = (p \ u \ w)^T$, with p being the pressure, and (u, w) the velocity components in physical space. E, G, G_1 and R, S, S_1 are respectively the convective and diffusive flux vectors at the plane (x, z) . [24]

Due to the absence of the pressure from the unknown variables' vector, it is impossible to relate the convective flux vectors with the unknown variables' vector (common problem in the incompressible flows). We don't prefer to introduce a new related equation among velocity and pressure variable because the construction of a fully implicit numerical scheme. [24] For these reasons we choose to introduce the artificial compressibility term, which allows to us the construction of a fully implicit methodology as well as a simple reverse of the matrix-coefficient of the unknown variables, in order to find the final desired values. So, the matrix [] after the addition of the artificial compressibility term takes the form:

$$[\Gamma] = \text{diag}\left(\frac{1}{S}, 1, 1\right)^T \quad (7)$$

After the addition of the artificial compressibility term, the equations (6) for incompressible flow are as follow:

$$\frac{\partial q}{\partial t} + \frac{\partial e}{\partial x} + \frac{\partial g}{\partial z} + r \cdot \frac{g_1}{z} = \frac{1}{\text{Re}} \left(\frac{\partial r}{\partial x} + \frac{\partial s}{\partial z} + r \cdot \frac{s_1}{z} \right) \quad (8)$$

where the symbols are the same as above.

The above N-S equations are the governing equations for unsteady flow. These are also used for the solution of steady flow fields. In these steady cases the time derivative is used for the construction of an iterative technique using the artificial time step in order to define our final steady state. We transfer the one solution (n) to the next "time level" (n+1), where we receive the final convergence of our problem in steady state setting simultaneously the time derivatives equal to zero.

The systems of equations for the flow problems consist of the two-dimensional incompressible Navier - Stokes equations after the addition of the pseudo-compressibility term (or artificial compressibility term), which take on a hyperbolic character with pseudo-pressure waves propagating with finite speed. In such types of problems "the information" inside the flow field is transmitted along its characteristic curves. In this sense we can relate the sign of eigenvalues with the upwind representation of the flow variables at the cell faces. The upwinding of the inviscid fluxes gives more freedom in devising implicit algorithms, since it loads up the diagonals of the implicit factors. Upwind differencing, also, alleviates the necessity to add and to tune the numerical dissipation for numerical stability and accuracy as the schemes with central differencing. [24] Here, we extend the FVS method for solving incompressible flow fields implicitly. In such flow fields the splitting of the convective flux vectors has to change sense because of their non-homogeneous property. The values of the flux vectors at the cell faces are approached by upwind schemes up to third order of accuracy. The unfactored discretized Navier-

Stokes equations are solved by an implicit second order accurate in time scheme, using Gauss-Seidel relaxation technique.

III. RESULTS

Three different domains with incompressible steady, laminar flows will be presented in order to estimate the recirculation zones inside them as well as the velocity and pressure distribution. We first present the numerical solution of a cavity flow with moving wall as a first approach. The following cases are the internal flows inside a channel with step as well as over a backward facing step. Although all the above domains have bounds on Cartesian grid lines, these are appropriate enough in order to prove the stability and chase out the accuracy of the refinement technique using the sequence of various rectangular sub-grids and our numerical scheme for the recirculation regions. The validation of our results is done by comparing the results with the correspondent ones of Cartesian uniform grid, with the same base grid size or of the literature ones.

D. Recirculating laminar flow around a square cavity with moving wall

The lid-driven cavity flow is the motion of a fluid inside a rectangular cavity created by a constant velocity of the upper side of the square domain, while the other sides remain at rest. Fluid flow behaviors inside these cavities have been the subject of extensive computational and experimental studies over the past years. Applications of driven cavities are in material processing, metal casting, pipelines flows, petroleum engineering applications, hydraulic systems etc. [29]

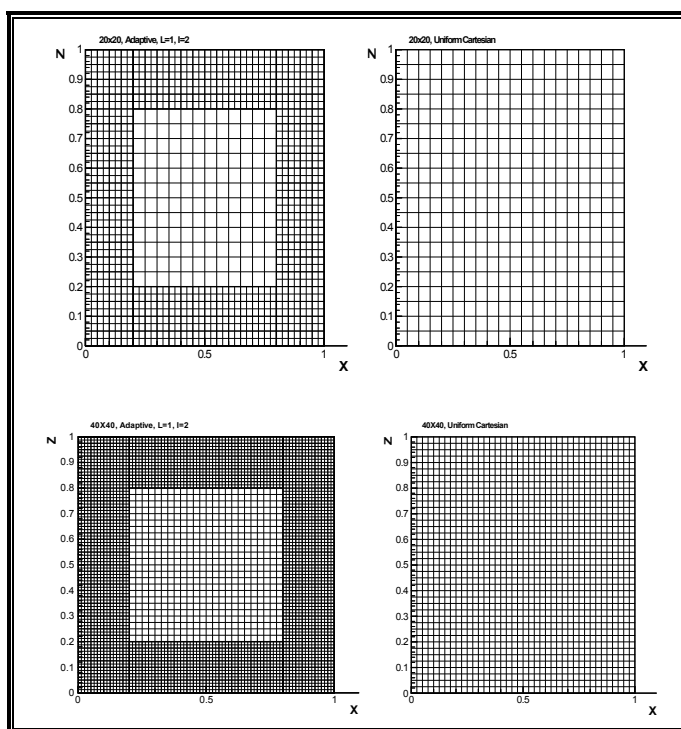


Figure 5: Uniform and nested grids for cavity flow (grid size: 20x20 or 40x40, $L=1$, $I=2$)

By the aforementioned flow field, we have the opportunity to test the independence and the accuracy of our refinement technique trying to prove that we can reduce the computational time and memory producing the desired accuracy simultaneously. In this case we don't face the geometry Cartesian approximation problem and we focus on the structured sub-grid block creation and implementation. Various grids have been used, uniform and block nested, in order to examine the effectiveness of our numerical scheme. The used numerical grids are presented in table I. The refinement has been applied close to the cavity walls, with one and two levels of refinement.

The Reynolds number is equal to 100 and 400. Some of the used numerical grids are presented in fig. 5, where we can see one level of refinement ($m=1$) and the refinement integer factor to be equal to 2 ($I=2$) for various grid sizes. The numerical simulation has been applied for 10x10, 20x20, 40x40 and 80x80 base grids. At figure 5 some of the uniform and block nested grids are presented, while at figure 6, the sub-grids for the cavity numerical solution are clearly stated and depicted. An important point during this numerical calculation is that the solutions must be transferred from the coarsest to the refine sub-grid choosing the appropriate velocity values according to the sub-grid location.

In table I, we present the computational times as well as the number of grid cells which have been used for each numerical solution. The reduction of the time is significant, which is achieved by the use of nested grids in comparison with the CPU time we need applying the uniform grids. For example using a nested grid 40x40 ($L=1$, $I=2$), we can achieve the accuracy of an 80x80 uniform one, reducing the computational time for almost 50% although the number of grid cells isn't much more different among the above two cases.

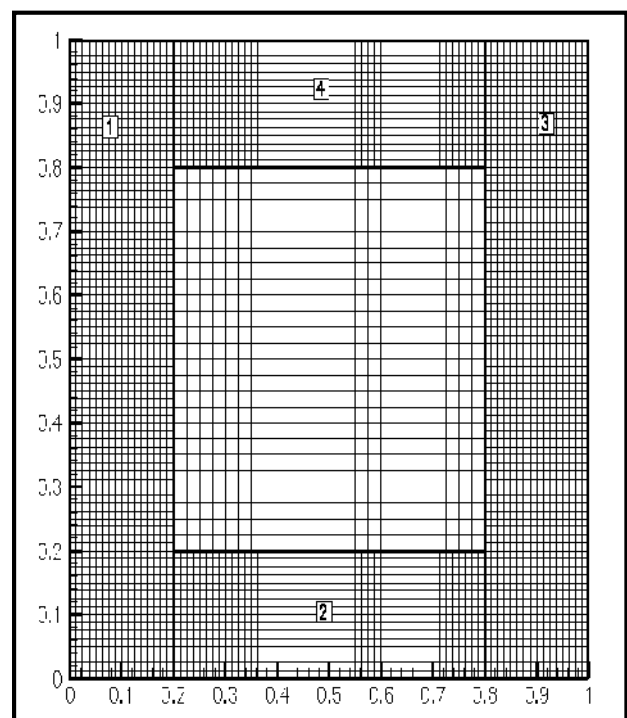


Figure 6: Four (4) sub-grids for the numerical estimation of cavity flow

It's interesting that in all the cases that we have applied the block – nested methodology, the computational time is significantly reduced in comparison with the application of uniform grids, although the accuracy of the results remains quite at the same level. (Table III)

The velocity values for the centre line of the cavity domain are presented in table III for several grid sizes, with or without refinement. By these results, we conclude that with the appropriate choice of grid levels we can achieve the accuracy at the regions of the numerical domain which demand more detailed approach (in this cases, we apply refinement near the walls of the cavity domain). However it seems that the way of boundary conditions application is appropriate and it doesn't affect the accuracy of the results by any negative way.

Table I: CPU time and number of computational cells

<u>Grid size</u>	<u>CPU time</u>	<u>Number of cells</u>
10x10, Uniform	2,42	100
10x10, L=1, I=2	6,2	292
20x20, Uniform	11,26	400
20x20, L=1, =2	42,46	1168
40x40, Uniform	84,53	1600
40x40, L=1, I=2	435,85	5696
80x80, Uniform	890,23	6400

Additionally, we can see that our approach is independent of the grid size, providing an appropriate accuracy for the flow variables. The accuracy of a refine grid is almost identical with those of a double sized uniform one as well as the accuracy of all the refined grids is appropriate. In order to test our numerical results and our algorithm concerning the independence of the grid size, we chose to develop a numerical solution using a 500x500 grid which we assume that it provides the “correct – accurate” solution. By this way we present the relative errors for the axial velocity values in table II. By these results, it seems that our solution is independent of the grid size, as well as that we can produce the desired accuracy using the block structured sub-grids with a significant reduction of computational time. Especially the relative errors at the case of 40x40 and 80x80 grid size are quite satisfied.

Finally we present the axial and vertical velocity distribution along the center line of the cavity in figures 7a and 7b as well as the vorticity lines in figure 8a for Reynolds number equal to 100 and at figure 8b for Re=800.

By these plots we conclude that the accuracy seems to be very satisfied again.

Table II: Errors for the axial velocity.

<u>Base grid size</u>	20x20	40x40	80x80
Uniform grid	1.70e-02	5.33e-03	5.02e-03
Level=1, I=2	1,61e-02	4.98e-03	4.97e-03
Level=2, I=2	1,56e-02	4.73e-03	4.71e-03

Table III: Velocity values for the centre line of cavity domain

<u>Grid size</u>	U_{\max}	Z_{\max}	W_{\max}	X_{\max}
10x10, Uniform	0,1877	0,4607	0,1532	0,8021
10x10, L=1, I=2	0,1927	0,4620	0,1535	0,8021
20x20, Uniform	0,1889	0,4620	0,1545	0,8021
20x20, L=1, =2	0,1930	0,4620	0,1681	0,8021
40x40, Uniform	0,1928	0,4620	0,1642	0,8018
40x40, L=1, I=2	0,1930	0,4620	0,1683	0,8021
80x80, Uniform	0,1935	0,4620	0,1647	0,8021

E. Flow Over a Backward-facing Step

The simulation and estimation of the flow over a backward-facing step is a classical problem in CFD. The main reason that this test case has been chosen is not only the appearance of an interesting industrial flow but also the close relationship of the specific case with the numerical modelling of the air in an urban environment which we intent to develop in our future research, and by this way we can validate our methodology. However this flow appears detachments and reattachment points [26] as well as recirculation zones and boundary layers which vary according to the aspect ratio, the expansion ratio or the Reynolds number of the flow.

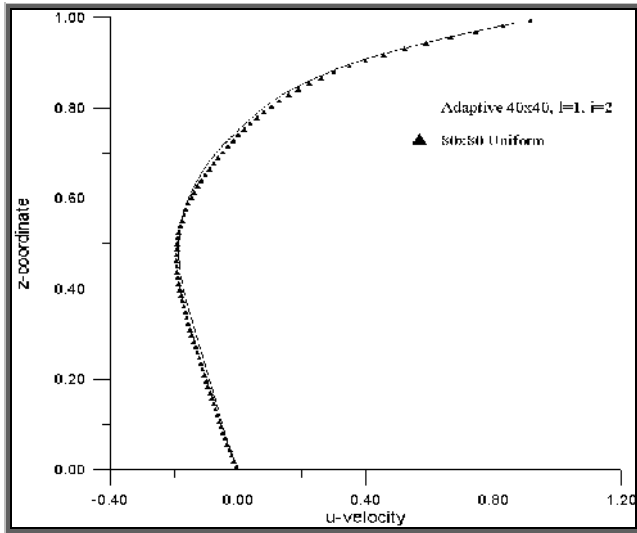


Figure 7a: Axial velocity profile for the cavity centre line, Re=100.

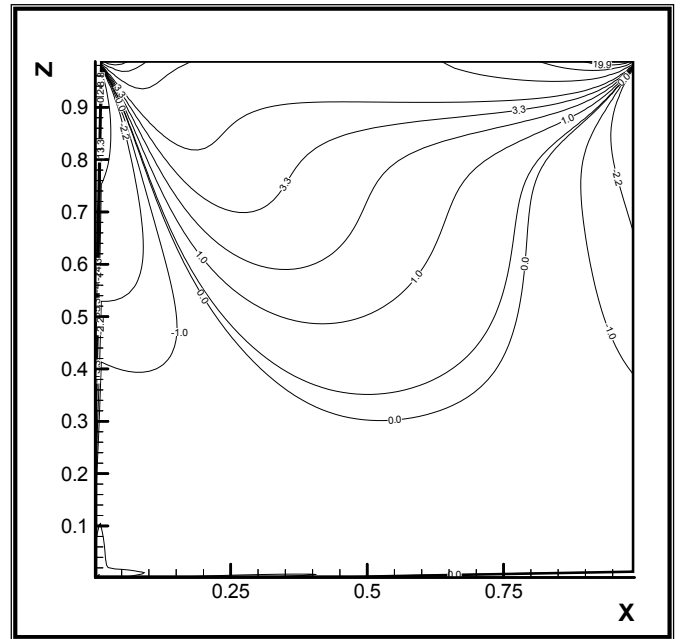


Figure 8b: Vorticity contours for the cavity flow, Re=400

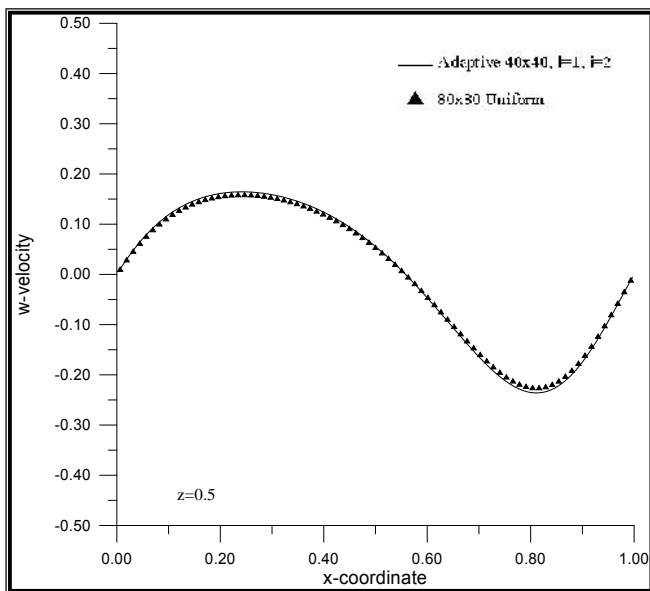


Figure 7b: Vertical velocity profile for the cavity centre line, Re=100.

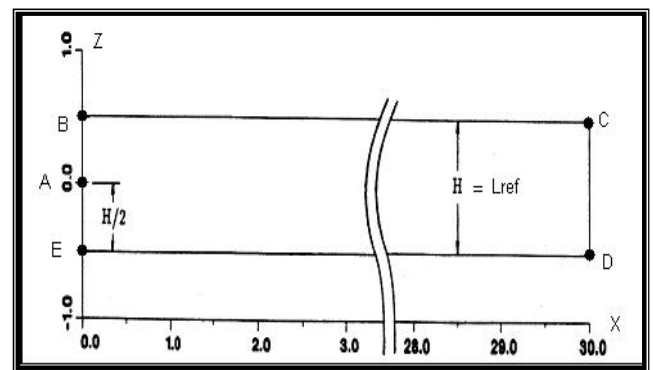


Figure 9: Physical domain of the backward – facing step channel.

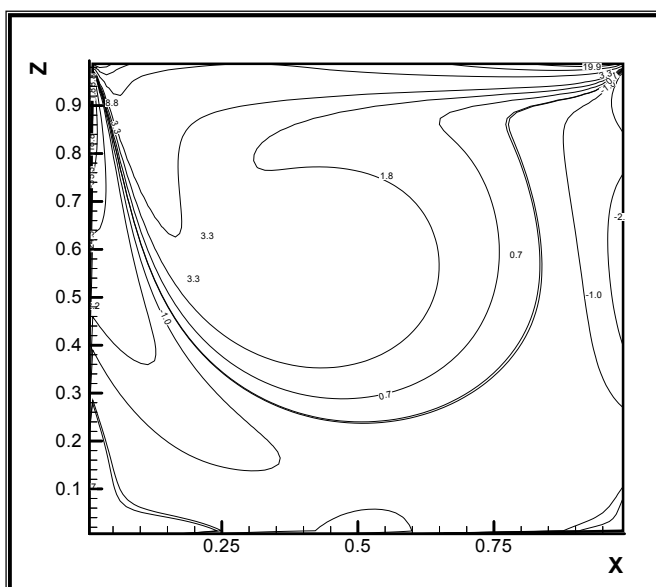


Figure 8a: Vorticity contours for the cavity flow, Re= 100

The expansion ratio is equal to 0.5 while all the variables are estimated with the reference length to be equal to the diameter of the cylinder. ($L_{ref}=H$)

The dimensionless pressure \tilde{p} is defined as below:

$$\tilde{p} = \frac{P}{\rho U_{ref}^2} \tag{9}$$

where P the pressure, ρ the density of the fluid and U_{ref} , the reference velocity which is equal to the average velocity to the inlet of the channel.

The grid generation and the numerical method that was described above were used for the calculation of steady flow inside a stenosed tube. The stenotic area is the 0.25% of the inlet area. The used numerical refinement grid is level=1 and I=2, (base grid: 401x26). The Re number, that was based on the maximum inlet velocity and the diameter of the

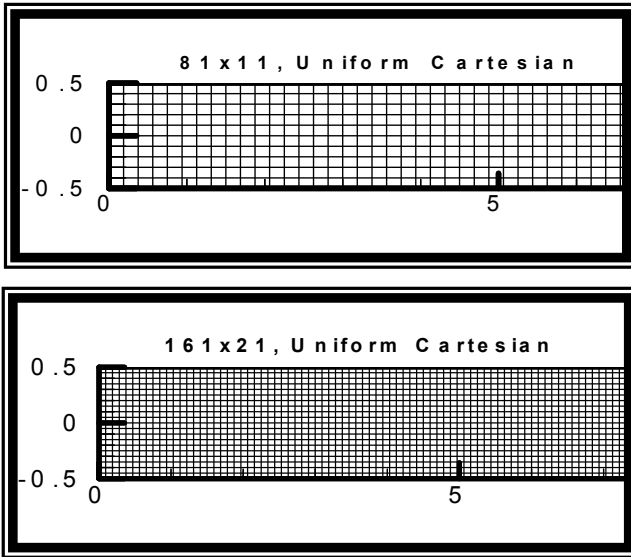


Fig.10a: Parts of the uniform Cartesian grids that have been used for the backward - facing step simulation and calculation

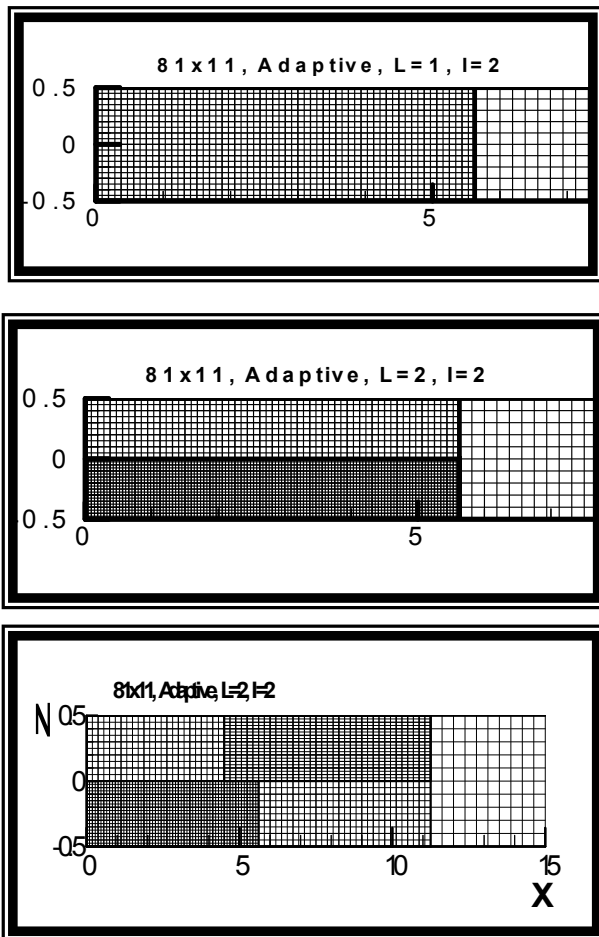


Figure 10b: Parts of the block bested Cartesian grids for the backward - facing step simulation and calculation, I=2.

inlet, was set equal to 400 as well as to 800. The boundary conditions are summarized as below, at table IV. It is worth to be mentioned that due to the below outlet boundary conditions, we need to choose the appropriate length of the cylinder; 15 dimensionless lengths for Re=400 and 30 ones for Re=800. In order to control the accuracy of the

proposed method, we simulated the current flow field by the use of two uniform grids sized 161x21 and 81x11 too. Finally we develop and use a Cartesian nested grid sized 81x11 with refinement factor equal to 2 using first only one and then two grid levels. The physical domain of the backward – facing step channel is presented in figure (9) while some of the used numerical grids or parts of these are presented in figure 10.

The recirculation lengths at upper and lower bound are presented at table V. It is obvious, by the aforementioned values, that the accuracy of 161x21 grid

Table IV: Boundary Conditions for the channel’s simulation

Upper bound, [BC]:	Wall conditions: $u = w = 0, \frac{\partial p}{\partial z} = 0$
Lower bound, [D]:	Wall conditions: $u = w = 0, \frac{\partial p}{\partial z} = 0$
Inlet, []:	Inlet conditions giving parabolic distribution of the velocity: $u = 24 \cdot z \cdot (0.5 - z), w = 0, \frac{\partial p}{\partial x} = 0$
Inlet, []:	Wall conditions: $u = w = 0, \frac{\partial p}{\partial x} = 0$
Outlet,[CD]:	Outlet conditions where the pressure has a value: $\frac{\partial u}{\partial x} = 0, w = 0, p = 0$

results is almost identical with 81x11 refine grid ones. Additionally we present Gartlings [32] relevant results where it seems that the convergence is quite satisfied. At table VI, we present the computational time as well as the number of the computational cells for each numerical grid that we have solved our domain. It is remarkable that although the block nested algorithms has comprised by larger number of cells than the uniform ones, the refine grid algorithm demands less computational time providing a higher accuracy of the results simultaneously.

Two velocity profiles along the flow field, upper and lower wall pressure distribution, as well as the pressure distribution are presented in figures (11), (12). The streamlines along the channel are presented at figure 13, for Re=800 using two levels of refinement.

By these results, it seems that the convergence between block nested algorithm results and uniform grid’s is very satisfied.

It’s worth mentioned that the results depicted by the block nested grid are accurate enough, present a very satisfied convergence with the according of the uniform grids as well as demand less computational time despite of the fact that

the number of computational cells has been increased. Additionally it was quite anticipated that the results of the block nested grid with 2 grid levels and refinement factor equal to 2 provides the best results, according to the literature ones, in an appropriate enough computational time. By various other test cases that we have developed, it seems that the usage of a larger refinement factor (for the specific flow problem), doesn't provide any improvement of the results. Consequently, it seems that the above grid size, the chosen refinement factor as well as the final number of sub-grids are a quite accurate choice providing the appropriate results for the flow variables. Additionally, in order to choose the location of the sub-grids, brief sub-routines have been developed, which they check the values of the u-axial velocity component during the numerical process. According to these velocity values as well as the criteria that we have set, we conclude to the final locations of the rectangular sub-grids. No problem has been raised by the

Table V: Recirculation data

$L_{ref} = H$ (fig .9)	Lower Wall Recirculation	Upper Wall Recirculation		
Grid Type	Recirculation length	Detachment point	Reattachment point	Recirculation length
Re=400				
161x21, Uniform cartesian	5.25	No detection	No detection	No detection
81x11, Uniform cartesian	5.33	No detection	No detection	No detection
81x11, Nested cartesian, l=1, I=2.	5.27	No detection	No detection	No detection
Re=800				
161x21, Uniform cartesian	6.10	4.87	10.37	5.50
81x11, Uniform cartesian	6.20	4.80	10.50	5.70
81x11, Nested cartesian, L=1, I=2.	6.10	4.85	10.40	5.55
Gartling, BFC, 400x20, [32]	6.10	4.85	10.48	5.63

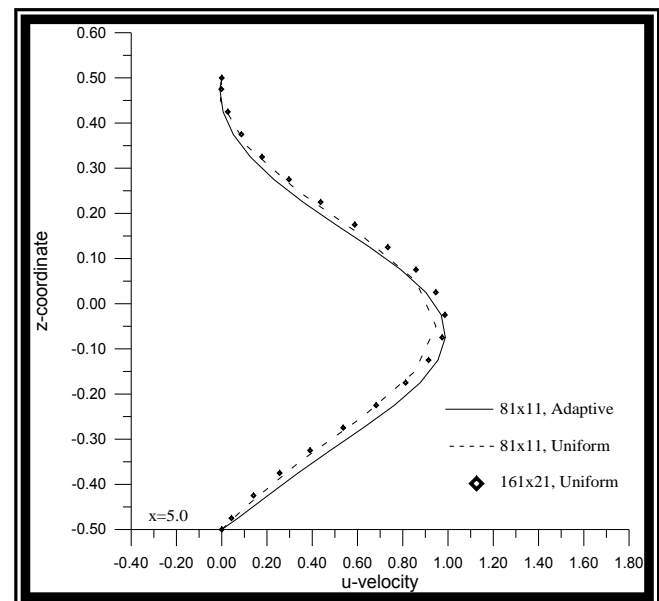
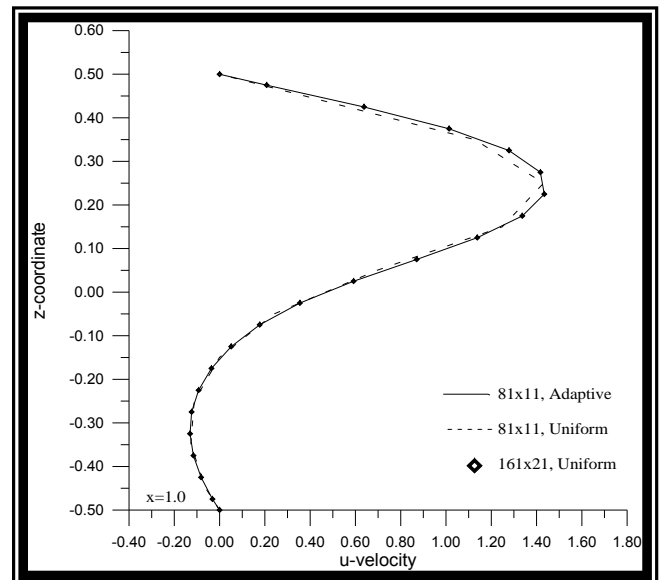
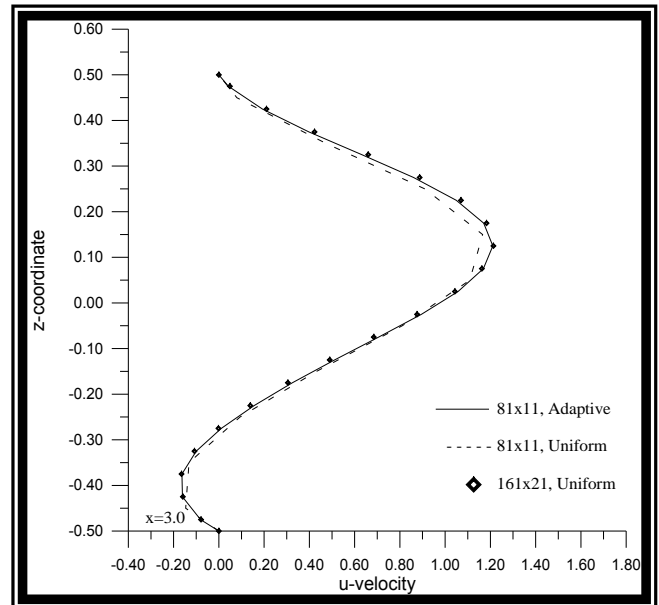


Fig. 11a: Velocity profiles along the channel flow field for various Cartesian grid sizes and types. Re=400.

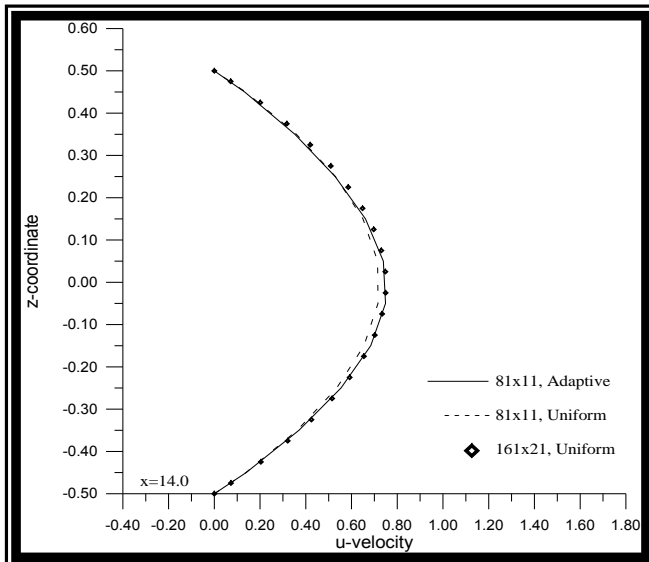


Fig. 11b: Velocity profiles along the channel flow field for various Cartesian grid sizes and types. Re=400.

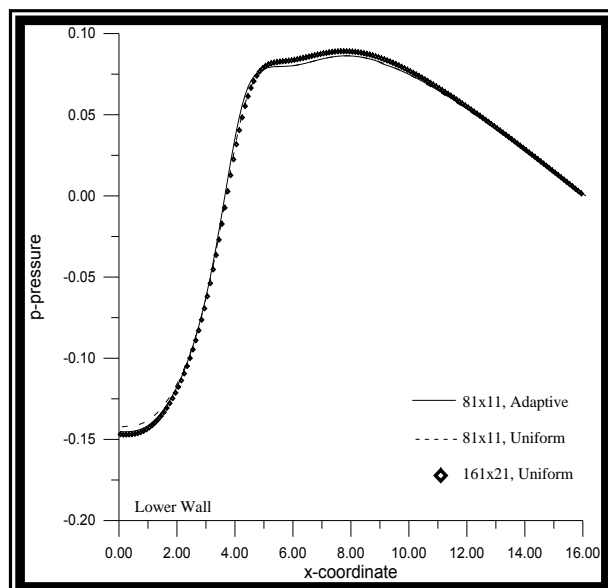
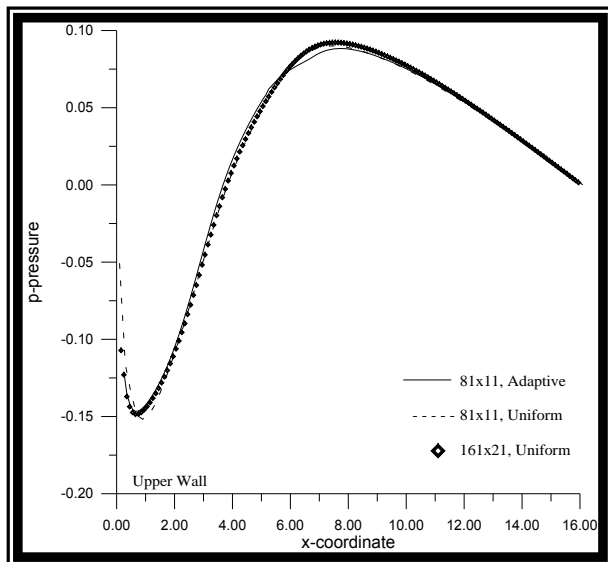


Fig. 12: Pressure distribution along the channel's walls

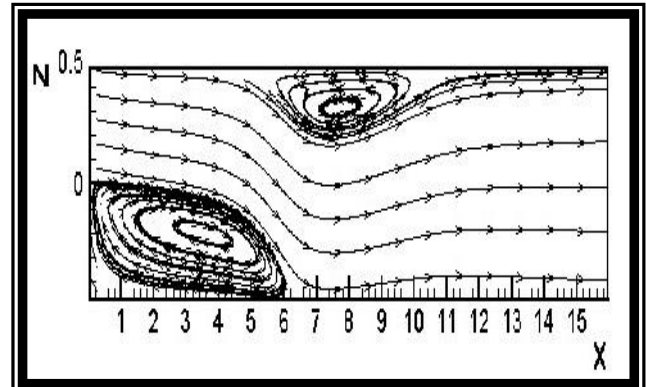


Fig.13: Streamlines along the channel. Grid size and type: block-nested 80x11, L=2, I=2. Re=800.

Table VI: CPU time & number of computational cells

<u>Grid size</u>	<u>CPU time</u>	<u>Number of cells</u>
Re=400.		
81x11, L=1, I=2	72,96	2172
81x11, uniform	23,01	891
81x11, L=2, I=2	120,03	4711
161x21, uniform	174,94	3381
Re=800.		
81x11, L=1, I=2	78,84	2172
81x11, uniform	32,46	891
81x11, L=2, I=2	131,97	5488
161x21, uniform	187,68	3381

transfer of the velocity or pressure values on the neighbouring bounds. Very important issue is to neglect the artificial cells when we solve between coarse – refine grids and use these only when we set the boundary values at the physical domains' bounds.

By this way, our numerical scheme provides accurate results for the flow variables of the physical domain with impressive reduction sometimes in computational time, as you can see at table VI. Especially in the cases of the geometries with very high aspect ratios, the reduction of the computational time is very important, without of course losing in the accuracy of the results.

F. Flow inside a channel with step

At the third test case, we will study and estimate the incompressible flow inside a channel with a step. Great importance in this test case is the estimation of the length of recirculation inside the cylindrical tube and the accuracy that is provided by the proposed nested algorithm. This test

case is an approach in order to prove that our methodology can be applied for the numerical solution of flows inside pipes even with high aspect ratios as sometimes we meet at industrial applications. Additionally we have the chance to study the various recirculation zones which are developed according to the Reynolds number as well as the geometrical ratios of the channel. The axisymmetric description of this test case, gives to us the opportunity to apply and test our nested refinement technique using symmetry boundary conditions. The physical domain is presented in figure 14.

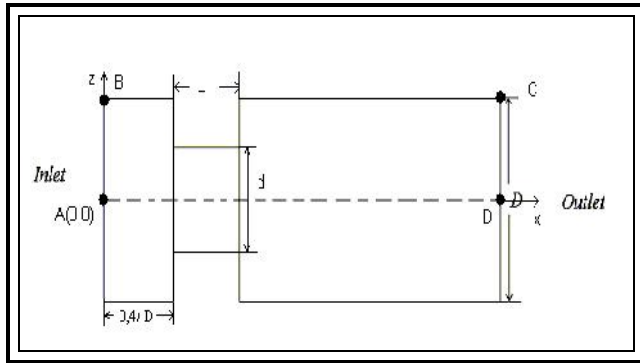


Figure 14: Geometry description of the channel with step

Although there are no curvilinear or complex bounds to the above geometry, we have to exclude some grid cells, if we want to estimate the flow with the appropriate accuracy. It seems that if we don't exclude these cells the provided solution is not the appropriate one. By this way we have three types of cells: the cells inside the flow of the channel, the cells which are outside of the channel and these must be excluded from the computational domain and finally the boundary cells.

Additionally, although we don't test the saw-tooth approach due to the Cartesian bounds, we verify the accuracy of our methodology according to the way of the application of the boundary conditions, especially to the areas that we have exclude cells.

The industrial application of the aforementioned channel are various, not only industrial engineering ones (power plants, water distribution channels etc) but also to the biomedicine area (arterial stenosis etc.).

In order to define the geometrical characteristics of the physical domain we have to obtain the diameters' ratio (internal d/external D), as these are presented in figure 14, as well as the aspect ratio of the channel (L/D). (Table VII) According to the above geometrical characteristics of the channel, the recirculation lengths are developed along it.

Table VII: Geometrical ratios of the channel

Grid size	d / D	L / D
61x21	0.8	0.4
101x21	0.6	0.6

For the grid refinement we have used 1 level of sub grids with integer factor equal to 2. Regarding the numerical

scheme for the N-S equations, the value of the artificial compressibility set equal to 1, as optimum choice for the reduction of the computational time. [25].

The inlet boundary condition at [AB] is:

$$u = 2 * (1 - z^2), w = 0, \frac{\partial p}{\partial x} = 0 \quad (10)$$

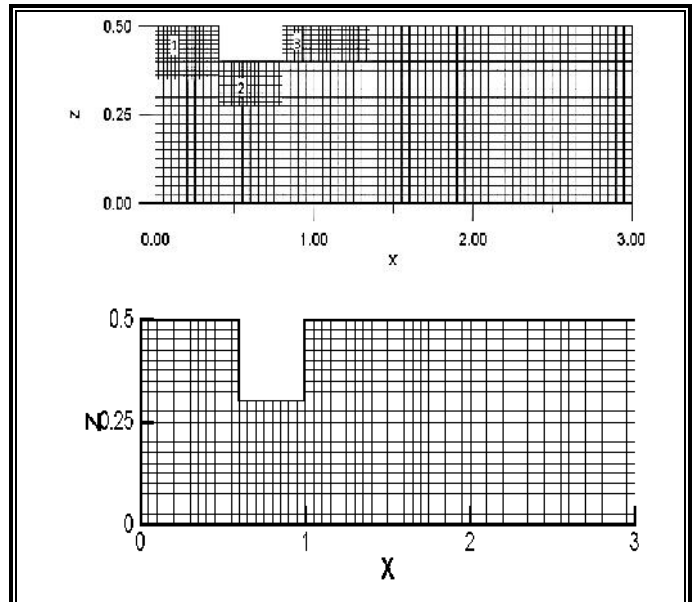


Figure 15: Parts of the numerical grids for the channel with step numerical solution, m=1, I=2.

where u is the axial component of the velocity of the fluid, p is the pressure and x,z are the Cartesian coordinates (fig. 15), while at the outlet boundary we give the pressure as you can analytically see to the below table VIII.

Table IX: Boundary conditions for the flow inside a channel with step

Upper limit [C]:	Wall conditions: $u = w = 0, \frac{\partial p}{\partial z} = 0$
Lower limit, [AD]:	Symmetry conditions: $\frac{\partial u}{\partial z} = 0, w = 0, \frac{\partial p}{\partial z} = 0$
Inlet, [AB]:	$u = 2 * (1 - z^2), w = 0, \frac{\partial p}{\partial x} = 0$
Outlet,[CD]:	$\frac{\partial u}{\partial x} = 0, w = 0, p = const$

Parts of the uniform and nested grids are presented at figure 15. Various results have been produced with very satisfied convergence. Four velocity profiles are presented in figure 16 along the channel, for various values of the geometrical

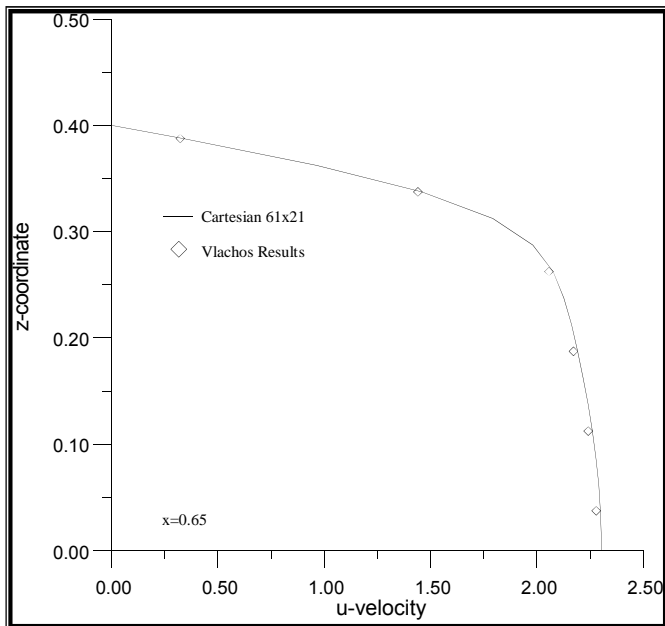


Figure 16a: Velocity profile along channel with step on $x=0.9$. Based grid size 61x21, $l/d=0.8$ and $d/D=0.8$

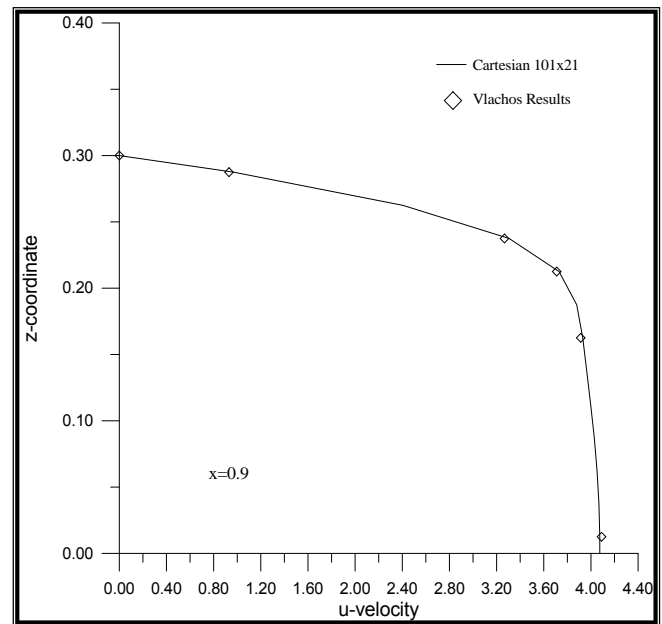


Figure 16c: Velocity profile along channel with step at $x=0.9$ (on the step). Based grid size 101x21, $l/D=0.6$ and $d/D=0.6$

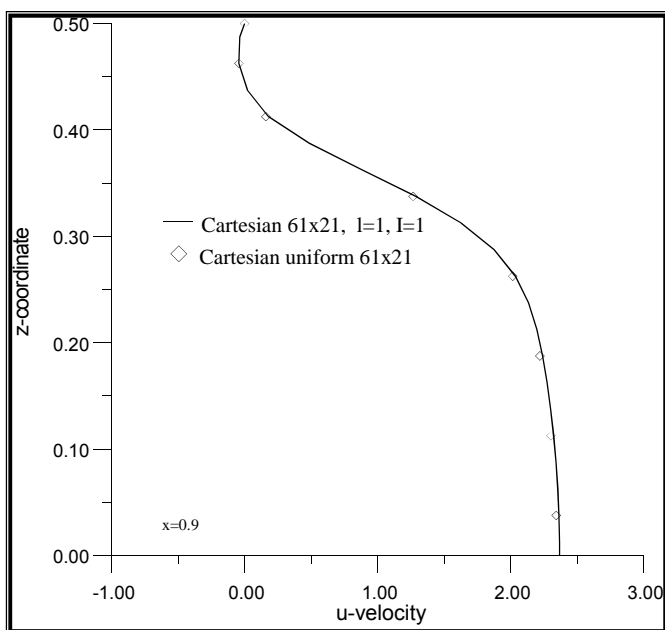


Figure 16b: Velocity profile along channel with step at $x=0.9$. Based grid size 61x21, $l/d=0.8$ and $d/D=0.8$

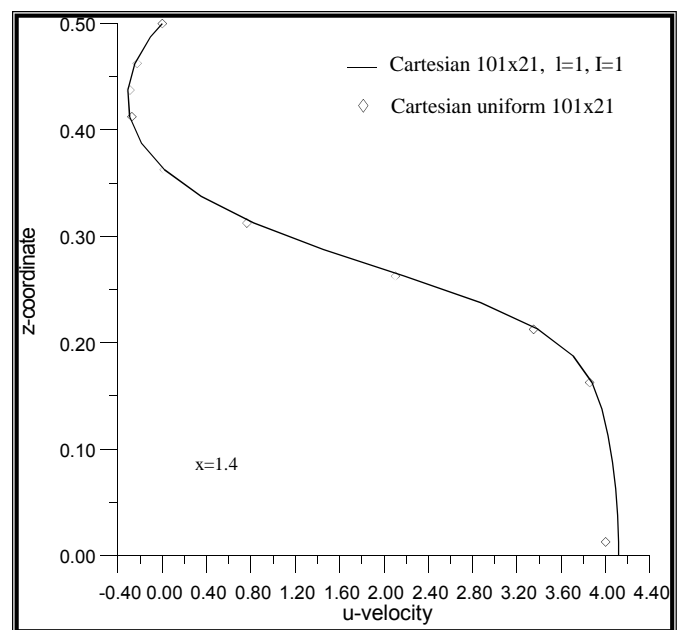


Figure 16d: Velocity profile along channel with step at $x=0.9$ (on the step). Based grid size 101x21, $l/D=0.6$ and $d/D=0.6$

ratios. The results present satisfied convergence. The comparison has taken place among uniform grid's and block nested grids results, for each case. Concerning the recirculation length, it seems that it is higher in the case of the channel with $d/D=0.6$ than the one with ratio equal to 0.8, as it was expected. By this way, the recirculation in this case is more intense. Finally the recirculation area has been estimated in both of the cases with high accuracy. The applications of the boundary conditions seem to be appropriate despite of the axisymmetric state of the flow. Good behavior is also providing through the neighbouring nested block grids.

IV. CONCLUSIONS

At the present paper we present a numerical approach for the prediction of recirculating flows. Concerning the discretization of the physical domain we apply a saw-tooth method while the final approximation of the geometrical bound is taking place by the use of only Cartesian grid lines. We generate uniform as well as refined Cartesian grids, using block nested structured sub-grids, where the numerical approach demands. We use a cell center discretization and

the boundary transfer is demonstrated in the interfaces by the use of interpolation for the velocity and pressure values at the coarse – fine interfaces of the refined sub – grids. The method is applied for steady, laminar, viscous and incompressible flows. We pay attention to the prediction of the recirculating lengths as well as the important points of each flow, in order to prove that our methodology is appropriate enough for the numerical estimation of pipeline's flows, sort or extended, providing the desired accuracy for various industrial applications. Main purpose of this paper is the testing and evaluating the above algorithm in order to be used for the numerical simulation of pipeline's flows. We present various numerical solutions using a variety of grid – sizes, refinement factors or sub-grids, and we prove that with the appropriate choice of the local sub-grids, we succeed high accuracy with an important reduction of the computational time simultaneously.

We have presented the numerical simulation of three flow fields of internal flows: flow inside a lid-driven cavity, the flow inside a backward-facing step as well as inside a channel with step. At all the above physical domains, we don't need to produce the Cartesian approximation of a curvilinear bound but we should evaluate the independence as well as the accuracy of our block – nested structured grid generator in combination with our numerical approach. Our results have been compared with those of uniform Cartesian grids as well as of the literature with very satisfied convergence. After these results it seems that our approach can be quite appropriate for the numerical simulation and estimation of pipeline flows without presenting any problem according to the domain discretization or the numerical schemes providing a satisfied accuracy concerning the recirculation characteristics of each flow fields. It is also quite encouraging that the way of boundary conditions application seems to be appropriate, between the neighbouring sub-grids without causing any problems in mass conservation. The prediction finally of the recirculation lengths as well as of the detachment and reattachment points is quite satisfied according to the literature results.

All the above numerical results, regarding the flow variables' values, computational time, and recirculation data prove that the Cartesian block refinement method is stable and accurate enough, and it can provide accurate modelling, simulation and results to recirculation zones of a pipeline flow domain for any industrial usage. The block Cartesian method is simple, it can be applied in any complex domain and provides accurate, grid independent, numerical solution for high aspect ratio geometries, as well as complex curvilinear domains, accomplishing also to reduce CPU memory and the simulation's computing time effort, advantages very important for an algorithm concerning industrial flow. With appropriate choice of local block refinement multilevel solutions computed with this algorithm can attain the accuracy of the equivalent uniform fine grid at less computational cost. Our next steps will be the development and application of the above methodology in pipeline flows with complex domains bounds, trying to produce the desired accuracy for the flow characteristics and variables.

REFERENCES

- [1] Louda P., Prihoda J., Kozel K., Svacek P., "Numerical simulations of flows over 2D and 3D backward facing inclined steps", *Int. Journal of heat and Fluid flow*
- [2] Louda P., Kozel K., Prijoda J., Benes L., Kopacek T., Numerical solution for incompressible flow through branched channel", *Comput. Fluids*, vol. 43, pp. 268-276, 2013
- [3] Wallin S., Johansson A.V., "A complete explicit algebraic Reynolds stress model for incompressible and compressible turbulent flows", *Journal Fluid Mechanics*, vol. 403, pp.89-132
- [4] Torres Maj., Garcia J., Numerical characterization of particle dispersion in the turbulent recirculation zones of sudden expansion pipe flows, *Proceedings of the 6th European conference on computational Fluid dynamics, Barcelona, 2014*
- [5] Lee T. and Mateescu D. Experimental and numerical investigation of 2-D backward-facing step flow. *Journal of fluids and structures*, vol. 12, pp. 703–716, 1998.
- [6] Armaly B., Durst F., Pereira J., and Schounung B. Experimental and theoretical investigation of backward-facing step flow. *Journal of fluid mechanics*, vol. 127, pp 473–496, 1983.
- [7] Manzan W., Vilela C., Mariano F., "Experimental and computational simulations of the flows over backward facing step", *Proceedings of 22nd Int. COBEM2013, SP, Brazil*
- [8] Santos R., Oliveira K., Figueiredo J., Influence study of the entrance channel in a two-dimensional backward-facing step flow, *Mecanica Computacional*, vol. XXIX, pp. 3347-3358, 2010
- [9] Kaiktsis L., Karniadakis G.E., and Orszag S.A. Onset of three-dimensionality, equilibrium, early transition in flow over a backward-facing step. *Journal of Fluid Mechanics*, 501–528, 1991.
- [10] Razavi S., Hosseinali M., A review of pressure behavior after a backward – facing step, *Recent advances in Fluid Mechanics*, pp. 52-58, 2009
- [11] Coirier, W.J. and Powell, K.G., "An accuracy assessment of Cartesian-mesh approaches for the Euler equations", *J. of Computational Physics*, Vol. 117, pp. 121-131, 1995
- [12] Georgantopoulou Chr.G., Pappou Th.J., Tsaggaris S.G., "Cartesian grid generator for N-S numerical simulation of flow fields in curvilinear geometries", *Proceedings of the 4th GRACM congress on comput. Mechanics*, pp. 526-534, 2002
- [13] Wang, Z.J., "A Quadtree-based adaptive Cartesian/Quad grid flow solver for Navier-Stokes equation", *Computers and Fluids*, Vol. 27, pp.529-549, 1998
- [14] Karai E., Kultari A., Haluk M., "Quad-tree based geometric – adapted Cartesian grid generation", *Recent Advances in continuum Mechanics, Hydrology and Ecology*, Vol. 1 pp. 15-25
- [15] Agresar, G., Linderman J.J., Tryggvason, G. and Powell, K.G., "An adaptive, Cartesian, front-tracking method for the motion, deformation and adhesion of circulating cells", *J. of Computational Physics*, Vol. 143, pp. 346-380, 1998
- [16] Lee J.D., Ruffin S., "Solution of Turbulent flow using a Cartesian grid based numerical scheme", *Recent Advances in Applied Mathematics and computational information sciences*, Vol.1, pp. 190-199
- [17] Pan D., Shen T., "A ghost cell method for the computation of incompressible flows with immersed bodies", *Proceedings of the 6th Int. conf. on Fluid mechanics and aerodynamics*, pp.78-87
- [18] Faldum E., Verzicco R., Orlandi P., Mohd-Yusof J., "Combines immersed-boundary finite-difference methods for three-dimensional complex flow simulations", *J. of Computational Physics*, vol.161, pp. 35-60, 2000
- [19] Ikeno T., Kajishima T., "Finite-difference immersed boundary method consistent with wall conditions for incompressible turbulent flow simulations", *J. of Computational Physics*, vol.226, pp. 1485-1508, 2007
- [20] Tseng Y., Ferziger J., "A ghost-cell immersed boundary method for flow in complex geometry", *J. of Computational Physics*, vol.192, pp. 593-623, 2003
- [21] Chr.G.Georgantopoulou, G.A.Georgantopoulos and S.Tsangaris, "Incompressible navier stokes equations solution using block nested Cartesian grid", *Proceedings of 25th ICAS2006, Humburg.*
- [22] Georgantopoulou Chr., Georgantopoulos G., Vasilikos N. and Tsangaris S., "Cartesian refinement grid generation and

- numerical calculation of flows around Naca0012 airfoil”
Proceedings of Int. Conference on Applied mathematics,
simulation, modeling, pp.256-263
- [23] Chr.G. Georgantopoulou and S. Tsangaris, “ *lock mesh refinement for incompressible flows in curvilinear domains*”, Applied Mathematical Modeling, Vol.31, pp2136-2148.
- [24] Berger M.J. and Collela P., “Local adaptive mesh refinement for shock hydrodynamics”, J. of Comput. Physics, Vol. 83, pp.64-84, 1989.
- [25] Pappou, Th. and Tsangaris, S., “*Development of an artificial compressibility methodology using Flux Vector Splitting*”, International J. for Numerical Methods in Fluid, Vol. 25, pp.523-545, 1997
- [26] Ospir D., Chereches C., Popa C., Fohanno S., Popovici C., “Flow dynamics in a double-skin façade, Proceedings of the 3rd WSEAS Int. conference on Finite differences, pp. 60-64
- [27] Bai X., Avital E., Williams J., “Numerical Simulation of a marine current turbine in turbulent flow”, Recent researches in Environment and Biomedicine, Vol. 1, pp.51-61
- [28] Shamloo H., Pirzadeh B., “Investigation of characteristics of separation zones in t-junctions”, Proc. Of Int. conference WSEAS on Water resources, Hydarulics and Hydrology, pp. 157-161, UK
- [29] Omari R., “CFD simulations of lid driven cavity flow at moderate Reynolds number, European scientific journal, vol. 9, pp. 22-35
- [20] Mavromatidis L., Michel P., Mankibi M. and Santamouris M., “Investigation of the sensibility of Multi-Foil insulations using the guarded hot plate and the guarded hot box test methods”, Palenc 2010, 5th Eur. Conf. on energy Performance (EPIC2010), 29 Sep.-1Oct, Rhodes island, Greece, 2010
- [31] Mavromatidis L., Michel P., Mankibi M. and Santamouris M., “Investigation of the contribution of multifoil insulation in the veduction of energy consumption of buildings”, 9th Geographical Conf., 4-6Nov, Athens, Greece, 2010
- [32] Gartling, D.K., “A test problem for outflow boundary conditions-flow over a backward-facing step”, Int. J. for Numerical Methods in Fluids, Vol.11, pp.953-967, 1990